



## ASSESSMENT OF NON-LINEAR AEROELASTIC BEHAVIOR OF AN AIRFOIL VIBRATION IN DYNAMIC STALL

D. A. Pereira<sup>1</sup>  
R. M. G. Vasconcellos<sup>2</sup>  
F. D. Marques<sup>1</sup>

<sup>1</sup>Engineering School of São Carlos – University of São Paulo, Laboratory of Aeroelasticity

<sup>2</sup>São Paulo State University, São João da Boa Vista

**Abstract.** *Stall-induced vibrations is a relevant aeroelastic problem affecting very flexible aero-structures. Helicopter blades, wind turbines, or other rotating components are severely inflicted to vibrate in stall condition during each revolution of its rotor. Despite of a significant effort to model the aerodynamics associated to the stall phenomena, non-linear aeroelastic behavior prediction and analysis in such flow regime remain formidable challenges. The purpose of this work is to present an aeroelastic analysis of a typical section in pitching subjected to stall-induced vibrations, which lead to limit cycles oscillations at higher angles of attack and complex non-linear features. The pitching-only typical section dynamics is coupled with an unsteady aerodynamic model based on Beddoes-Leishmann semi-empirical approach to produce the proper framework for gathering time series of aeroelastic responses. The analyses are performed by checking the content of the aeroelastic responses prior and after limit cycle oscillations occur. Evolutions on limit cycles amplitudes are used to reveal bifurcation points. Analyses in frequency domain also provide important information to assess, characterize, and qualify the nonlinear behavior.*

**Keywords:** *Aeroelasticity, dynamic stall, nonlinear vibrations, stall-induced vibrations, time series analysis, bifurcations.*

### 1. INTRODUCTION

Aeroelastic problems related to stall-induced vibrations represent great challenge in modeling and analysis. These problems may lead to highly non-linear phenomena, when the unsteady aerodynamics gives a major contribution to the aeroelastic system complexity. Helicopter industry is always aware of the complex effects of stall-induced vibrations, since the helicopter blades are constantly subjected to the effect of dynamic stall per rotor revolution, particularly in forward flight (Bramwell *et al.*, 2001; Leishman, 2006; Bielawa, 2006). In wing energy industry, modern blade design (slender shapes) and pitching control approaches may induce severe blade reactions at dynamic stall regime (Burton *et al.*, 2001; Hansen, 2008). For unsteady aerodynamic modeling, the non-linear flow effects of interest are mostly due to separated flows and compressibility effects leading to the appearance and dynamic excursion of shock waves. Their modeling is particularly difficult because of the lack of complete understanding on some physical aspects of unsteady flows; for example, separation and turbulence mechanisms. For aeroelastic applications, the ideal and, perhaps, most general aero-structural model would be based on solutions of the non-linear fluid mechanics equations, which considers unsteady, compressibility and viscous effects, simultaneously with the solution of the equations of motion. The instantaneous states, which are generated by each of the corresponding equations, would be exchanged and the global simultaneous solution would produce both aerodynamic response and structural motion histories, which depend on the given initial conditions (Marques, 1997).

The problem in applying the general aeroelastic model is mainly related to the unsteady aerodynamic model in use. Solutions to the non-linear fluid mechanics equations have been the focus of a great amount of research effort. For practical applications, however, solutions of the general fluid mechanics equations can usually be attained only by means of numerical techniques, or computational fluid dynamics (CFD) methods (Edwards and Thomas, 1989; Anderson, 1991), that normally demand extensive computations. These methods encompass any numerical technique for specific fluid mechanics applications. For instance, finite-difference, finite volume, and finite element techniques are frequently used in numerical solutions in fluid mechanics applications. Limitations of CFD methods are basically the ones concerning the great amount of computations required.

Alternative models of non-linear unsteady aerodynamics for aeroelastic applications have been achieved on the basis of some essential assumptions. Primarily, in aeroelastic models, the decoupling between the fluid mechanics equations and the equations of motion is an assumption that eliminates the need for simultaneous solution of the combined aero-structural set of equations. Therefore, by this premise the unsteady aerodynamic model is determined in isolation of the physical laws governing the structural motion. An intrinsic element of this decoupling process is that any alternative unsteady aerodynamic response model should account for the spatio-temporal behavior of the internal aerodynamic states.

Formal mathematical approaches to determine the functional relationship of the hereditary behavior of unsteady aerodynamic responses, are originally due to the use of the superposition principle over transient responses to step changes, namely, indicial responses (Tobak and Pearson, 1964; Tobak and Chapman, 1985; Etkin and Reid, 1996). This approach,

which provides exact representation of the linear unsteady aerodynamic behavior, is categorized as a functional due to its dependence on the complete (or partial) motion histories. However, practical use of the resulting complex integral equations is only permitted by simplifications, for example, by replacing the mathematical description of the motion history by its Taylor series expansion, or by assuming a limited dependence on the motion past values. Other functional forms; for instance, the Volterra series (Silva, 1993a,b) also provide appropriate frameworks to the production of non-linear unsteady aerodynamic functionals.

Semi-empirical methods, or phenomenological models, comprise a class of aerodynamic models based on the premise of modeling unsteady flow response by considering its functional relationship with respect to the motion histories. Indeed, most of the knowledge on unsteady flow behavior is due to experimental work, and basically, semi-empirical models use the information from these experiments to establish a mathematical and logic formulation of the events that determine the unsteady aerodynamic response over a range of incidence motions and flow regimes. The works by Tarzanin Jr. (1972), Beddoes (1976), Beddoes (1982a), Beddoes (1982b), Tran and Petot (1981), Leishman and Beddoes (1989), and Mahajan *et al.* (1993), are examples of contributions to semi-empirical modeling. The nature of semi-empirical methods facilitates their incorporation into aeroelastic stability and control design. In addition, semi-empirical methods have the advantage of being computationally fast. Nevertheless, semi-empirical models need extensive, specific and precise experimental data. There is also the problem of correlating this data with mathematical and logic formulations.

The Beddoes-Leishman model (Beddoes, 1976, 1982a,b; Leishman and Beddoes, 1989) is a very popular choice of dynamic stall model for helicopter industry, as well as for most recent analyses in wind energy applications. Nonetheless, the Beddoes-Leishman approach is also more complex compared to other semi-empirical models. It is based originally based on convolution of indicial response functions because of more effective computational formulation. To account for the flow physics involved in the dynamic stall phenomenon, this approach includes contributions to each stage when important separated flow events occur. Original Beddoes-Leishman model considers the effects of trailing edge separation, vortex flow (dynamic stall effect), and flow reattachment when rebuilding lower angles of attack. Compressibility effects are also incorporated to this approach as it is significant to the helicopter blade unsteady loading, however, for the most recent applications to wind turbine blades, novel formulations have been developed neglecting the Mach number influence (Hansen *et al.*, 2004; Chantharasenawong, 2007).

The purpose of this paper is to present the assessment of non-linear aeroelastic behavior due to stall-induced unsteady aerodynamic loading. The investigation has been carried out using 1-*dof* typical section in pitching motion and dynamic stall model based on Beddoes-Leishman approach (Beddoes, 1976, 1982a,b; Leishman and Beddoes, 1989). Basic analyses are performed by inspecting the time series from aeroelastic responses. Non-linear behavior due to bifurcation and complex harmonic coupling in limit cycle oscillations are also investigated.

## 2. AEROELASTIC MODEL

The aeroelastic model is based on typical section for only pitching motion admitting large angles of attack. To take into account the effects of separated flow around the airfoil the Beddoes-Leishman dynamic stall model is used (Beddoes, 1976, 1982a,b; Leishman and Beddoes, 1989). Structural behavior are admitted as linear with variables that ensure proper nonlinear aeroelastic dynamics with realistic-valued parameters. Further investigation is planned to experimentally validate the approach related to this work. More details on the aeroelastic model are presented in the following sections.

### 2.1 Aeroelastic equation for pitching airfoil

Pitching-only typical aeroelastic section of chord  $c$  is adopted. Linear 1-*dof* structural dynamics depend on the pitching spring stiffness and inertia moment around the elastic axis. The Beddoes-Leishman model is used to calculate the unsteady aerodynamic loading of the airfoil under separated flow effects at higher angles of attack.

Aeroelastic 1-*dof* equation of motion is given by,

$$I_\alpha \ddot{\alpha} + k_\alpha \alpha = M_{ea} \quad , \quad (1)$$

where  $\alpha$  is the pitching angle (angle of attack),  $I_\alpha$  is the inertial moment,  $k_\alpha$  is the pitching spring stiffness, and  $M_{ea}$  is the pitching moment (positive for airfoil leading edge up).

A convenient way to represent the equation of motion can be with non-dimensional form. Therefore, for the pitching natural frequency,  $\omega_\alpha = (k_\alpha/I_\alpha)^{\frac{1}{2}}$ , the radius of gyration,  $r_\alpha^2 = \frac{I_\alpha}{mc^2}$ , and the mass ratio,  $\mu = \frac{4m}{\pi\rho c^2}$ , where  $m$  is the airfoil mass for unit length,  $\rho$  is the air density, the non-dimensional form of the aeroelastic equation results,

$$\ddot{\alpha} + \omega_\alpha^2 \alpha = \frac{4V_\infty^2}{r_\alpha^2 \mu \pi c^2} C_{m_{ea}} \quad , \quad (2)$$

where  $V$  is the airspeed and  $C_{m_{ea}}$  is the pitching moment coefficient with respect to the elastic axis.

For the purpose of aeroelastic simulation, Eq. (2) can be integrated in time with any conventional numerical method. Here, the Runge-Kutta approach is considered.

## 2.2 Nonlinear aerodynamic model

This paper considers the original formulation of the Beddoes-Leishman model (Beddoes, 1976, 1982a,b; Leishman and Beddoes, 1989). This model deals with the prediction of dynamic stall, thereby accounting for non-linear unsteady aerodynamic effects due to separated flow fields surrounding airfoils. Original Beddoes-Leishman model considers leading edge separation and impulse forces for compressibility effects (although the airspeed range under consideration for this work will not reach Mach numbers higher than 0.4). The Beddoes-Leishman model admits three contributions to the total loading, namely: (i) unsteady attached flow loading; (ii) trailing edge separation effect; and (iii) dynamic stall or vortex flow effect. General aspects of each contribution are presented in the following paragraphs. For more detailed information on Beddoes-Leishman model the reader must refer to Beddoes (1976, 1982a,b); Leishman and Beddoes (1989).

The unsteady attached loading is computed using changes in aerodynamic forces with respect to a step change in airfoil pitch angle or pitch rate, the so-called *indicial aerodynamic responses*. These indicial lift functions can be expressed in terms of exponential functions in non-dimensional time likewise Wagner function classical approximations (Fung, 1955; Bisplinghoff *et al.*, 1996). Therefore, lift transfer function can be derived straight from the indicial function, which facilitates the numerical solution for arbitrary loading terms using superposition assumption of a step inputs set. This means that Duhamel's integral formulation can be applied and the indicial lift coefficient response is given by:

$$C_L(s) = C_{L\alpha}(s) \left[ \alpha(0)\phi(s) + \int_0^s \frac{d\alpha(\sigma)}{ds} \phi(s - \sigma) d\sigma \right], \quad (3)$$

where  $s = (2V_\infty t)/c$  represents the non-dimensional time (relative distance travelled by the airfoil in terms of semi-chords),  $\alpha(0)$  is the angle of attack initial condition, and  $\phi(s)$  is the indicial response function.

The indicial response function can be written in a convenient way so that compressible and time-delay effects are accounted into the model (Beddoes, 1982a). A simplified representation of this assumption is,

$$\phi(s') = \phi_c(s') + \phi_I(s') + \phi_q(s') \quad , \quad (4)$$

where  $s' = s(1 - M^2)$  is the non-dimensional time parametrized by the Mach number ( $M$ ),  $\phi_c(s') = 1 - A_1 e^{-b_1 s'} - A_2 e^{-b_2 s'}$  is the circulatory component ( $A_{1,2}$  and  $b_{1,2}$  are real-valued constants),  $\phi_I(s') = (4/M)e^{-s'/T_I}$  is the impulsive component ( $T_I$  is a time constant – first-order system delay), and  $\phi_q(s') = (-1/M)e^{-s'/T_q}$  is the impulsive component of the indicial lift response to pitch rate about 3/4 chord ( $T_q$  is respective time constant).

Trailing edge separation effects are assessed with the Kirchhoff theory (Thwaites, 1960). This approach can be used to quantify the associated loss of circulation with the progressive trailing edge separated flow. Circulatory component of the lift coefficient can be corrected with,

$$C_L = 0.25 C_{L\alpha} \alpha \left( 1 + \sqrt{f} \right)^2 \quad , \quad (5)$$

where  $f$  is the separation point with respect to the airfoil chord, as function of airfoil incidence and empirical parameters.

The final contribution to the unsteady aerodynamic loading is related to the effects of deep stall regime (McCroskey, 1982). This highly non-linear dynamics is related to vortex shedding intensified by trailing edge separation progress up to the release of leading edge vortices. The physical events associated to this flow regime are complex and an acceptable modeling requires precise understanding of them. Several stages in the physical events related to dynamic stall can be observed. Admitting progressive increase in airfoil incidence and after reaching the static stall in the lift curve (beyond the limits imposed by Kirchhoff theory), separation delay effects start to dominate. The separation delay leads to the continuation of linear increase in lift, which goes beyond the static stall angle. Moreover, during lift increment beyond static stall the unsteadiness of the shed circulation at high angle of attack results in lift reduction and adverse pressure gradients. Because of adverse pressure gradients, additional unsteady effects rise in the form of attached flow reversal. All these events result in a lag effect in the boundary layer that ultimately provide conditions to the onset of leading edge separation.

Leading edge separation starts a vortex departing and shedding toward trailing edge. Pressure gradient by this convected vortex leads to lift overshoot, sometimes as significant as 50 to 100% of the static maximum lift, and this generated lift is also called stall or vortex lift. This large contribution from the upstream moving vortex also gives rise to nose-down pitching moment. Then, when the vortex reaches the trailing edge the entire upper surface of the airfoil is under separated flow.

As pitching moment reduces significantly at stall lift condition the airfoil motion will be experience angle of attach reduction (it may also be prescribe as in pitching adjustments per revolution like in helicopter blades in forward flight). When the angle of attack is low enough, flow reattachment is possible. The reattachment occurs within a large amount of dynamic lagging effects. The reasons for that are due to flow reorganization from the fully separated regime, and by a reverse kinematic induced camber effect on the leading-edge pressure gradient by the negative pitch rate. As result fully reattached flow around the airfoil is only reached below the static stall angle, introducing a large amount of hysteresis to the unsteady loads.

The Beddoes-Leishman model uses a practical approach to account to the vortex shedding process. The stall or vortex lift is modeled assuming the increment in lift during vortex shedding in terms of the difference between instantaneous linear value of circulatory lift ( $C_L^c$ ) and the corresponding lift as given by the Kirchhoff theory, that is,

$$C_V = C_L^c \left[ 1 - \frac{(1 + \sqrt{f})^2}{4} \right], \quad (6)$$

where  $f$  as in Eq. (5).

Simultaneously, the total vortex lift is allowed to decay exponentially with time, but incremented in value. This is considered so that when lower lift rate of change occurs the vortex lift is rapidly dissipated. The lift exponential decay is given as,

$$C_L^v(t) = C_L^c(t-1)E_v + [C_V(t) - C_V(t-1)]\sqrt{E_v}, \quad (7)$$

where  $E_v = e^{(-\frac{c}{2T_v} \frac{\Delta t}{V_\infty})}$ , for  $T_v$  denoting a time constant.

### 3. RESULTS

The aeroelastic model admitted in this study presents parameters as given in the Table 1. Moreover, NACA0012 airfoil is considered to adjust the unsteady aerodynamic model.

Table 1. Aeroelastic parameters.

Parameter	Value
chord length, $c$	0.3 m
air density, $\rho$	1.225 kg/m <sup>3</sup>
elastic axis position	0.3 (% $c$ )
mass ratio, $\mu$	11.5486
pitching frequency, $\omega_\alpha$	2 Hz
radius of gyration, $r_\alpha$	0.3

For a range of 0.0 to 70.0 m/s, simulations have been performed to assess non-linear response since limit cycle oscillations (LCO) regime are expected. Simulations are carried out adopting an initial condition in angle of attack followed by leaving the aeroelastic system to react. An evolution with respect to airspeed reveals the condition in which limit cycle oscillation occurs. Figure 1 illustrates the LCO amplitude progress for simulations that admits initial angle of attack of  $\alpha_0 = 20^\circ$ . The LCO behavior onset can be observed near 23.8 m/s, thereby indicating bifurcation phenomenon.

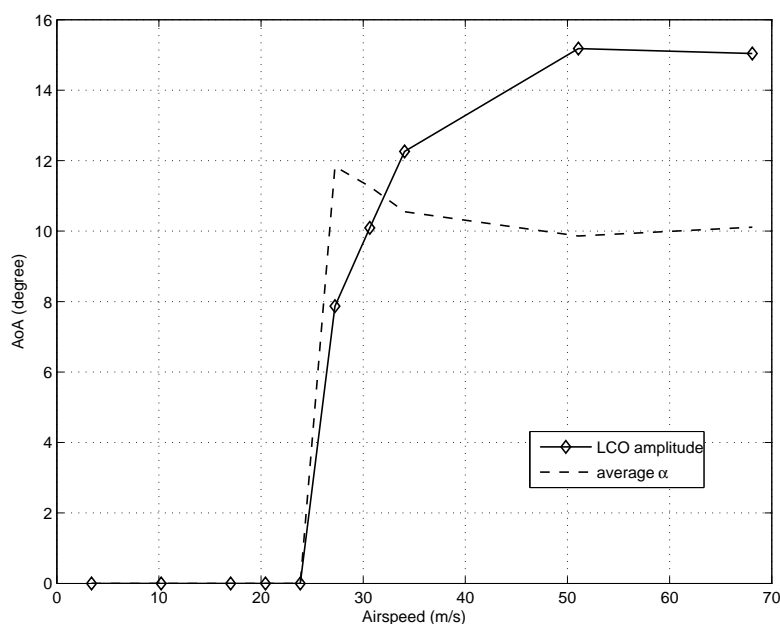


Figure 1. LCO amplitudes evolution with respect to airspeed ( $\alpha_0 = 20^\circ$ ).

These LCOs after bifurcation point are all due to stall-induced excitation, which restricts the motion at higher angles of attack. As an example of such responses, Fig. 2 reveals oscillation trapped at high angles of attack, thus in LCO condition,

with average angle of  $\approx 10^\circ$  and amplitude of  $\approx 15^\circ$  at  $V_\infty = 51.1 \text{ m/s}$ . A reasonable explanation for this condition can be related to loading degeneration due to dynamic stall at highest angles of attack and subsequent unsteady loading recovering due to reattached flow effects when traveling in lower airfoil incidence angles.

Therefore, at LCO condition the resulting amplitude in Fig. 1 are with respect to average angle of attack values given by the dashed line. Obviously, transient dynamics are not considered here.

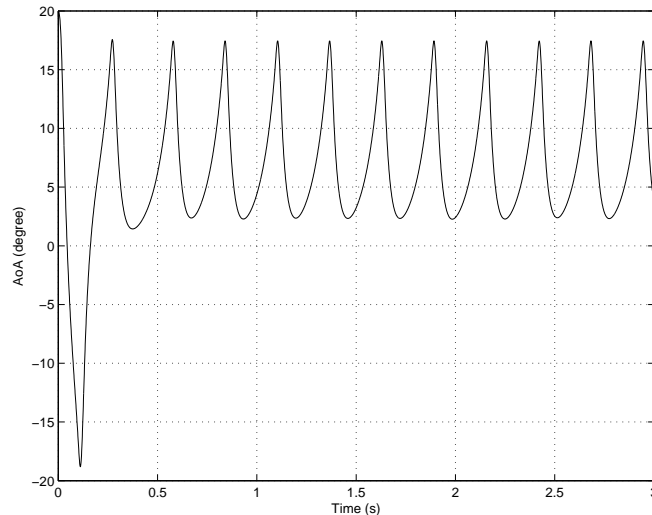


Figure 2. LCO at high angle of attack induced by stall ( $\alpha_0 = 20^\circ$ ,  $V_\infty = 51.1 \frac{\text{m}}{\text{s}}$ ).

As non-linear behavior has been reached, it is reasonable to check LCO in terms of its stability. A straightforward way to verify stability can be by simulating the system with different initial conditions and how the responses lead to LCOs. This procedure has been performed for a fixed airspeed ( $V_\infty = 51.1 \frac{\text{m}}{\text{s}}$ ) and the resulting LCOs for  $\alpha_0$  equals to 5, 20 and  $45^\circ$  are depicted in Fig. 3. Here, the phase portrait of pitching motion indicates that all  $\alpha_0$  initial values results in the same LCO responses. Stability is guaranteed since LCO can be reached from both sides (internally and externally). The same procedure has been performed for other airspeeds within the range of LCO existence, and for all cases stability is observed.

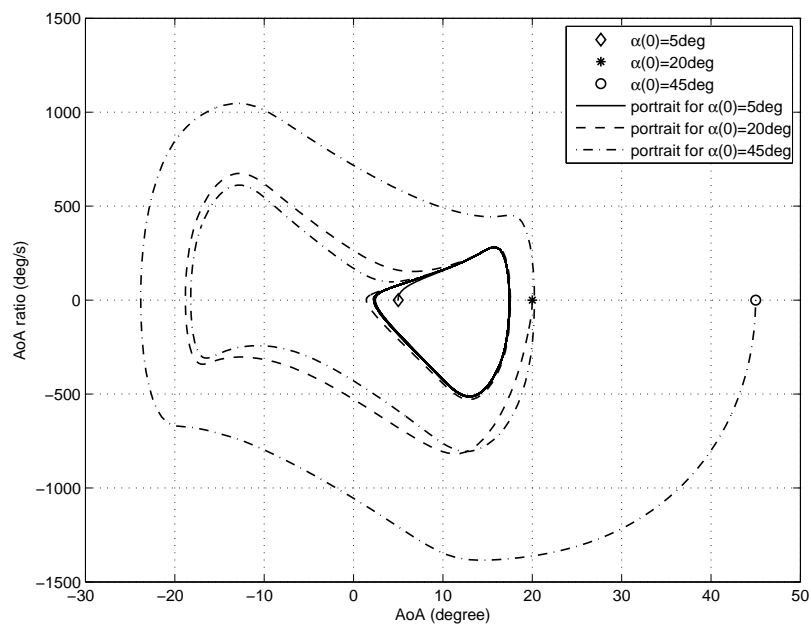


Figure 3. Phase portrait for a stable LCO (different initial condition  $\alpha_0$ ,  $V_\infty = 51.1 \frac{\text{m}}{\text{s}}$ ).

The existence of bifurcation leading to LCO response allows inferring that exists a fundamental LCO frequency with its respective harmonics. This complex frequency distribution can be computed and observed from Fourier analysis of the respective time series. As non-linear aerodynamics plays an important role on the frequency content on LCO condition, it is reasonable that variations with respect to airspeed can occur. To help understanding how airspeed contributed in

the frequency content and harmonics distribution after bifurcation, time-frequency analysis can be used. Figure 4 shows concatenated time history windows of same size at different increasing airspeeds. Here, the airspeeds are, 3.4, 10.2, 17.0, 20.4, 23.8, 27.2, 30.6, 34.0, 51.1, and 68.1  $m/s$ , respectively to each distinct time window in Fig. 4. As transient responses are neglected, thus each time window is related to steady state dynamic responses. Figure 4 also shows a spectrogram (Kantz and Schreiber, 2004) closely related to the time windows per airspeeds. For each time window the frequency content can be observed in the spectrogram. It is clear to observe the harmonic coupling for the LCO conditions after bifurcation. Moreover, harmonic frequencies are also affected by increasing airspeed, when there is a trend of increasing the fundamental LCO frequency.

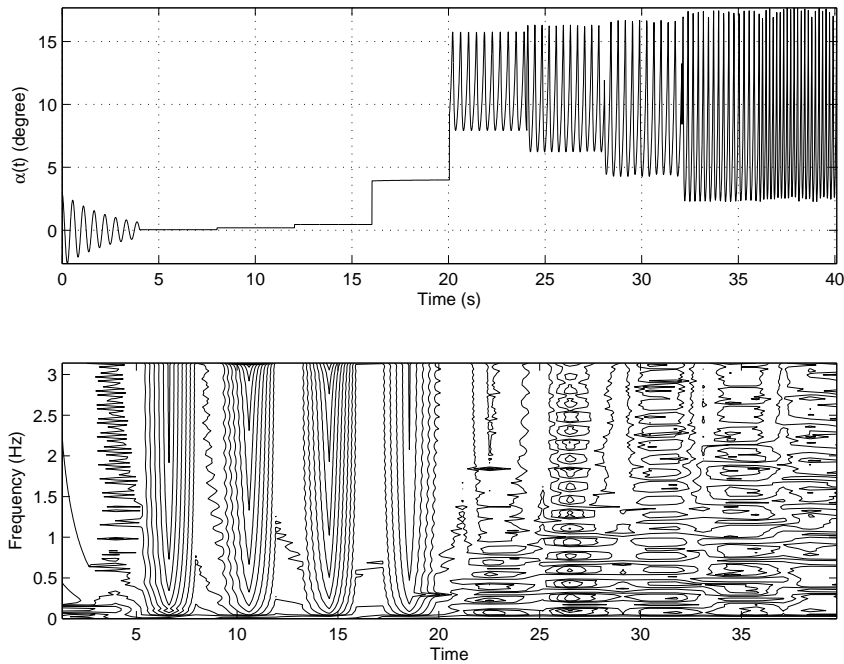


Figure 4. Concatenated time windows of increasing airspeeds and spectrogram ( $\alpha_0 = 20^\circ$ ).

Complementary to the spectrogram analysis, for established LCO conditions, FFT can be used to observe the fundamental and respective harmonics per airspeed. Resulting power spectra at 27.2, 30.6, 34.0, 51.1, and 68.1  $m/s$  are presented in Fig. 5. As reference to a stable equilibrium condition, the spectrum for  $V_\infty = 3.4 m/s$  is depicted in the same Fig. 5 (dashed line). In this case, unique fundamental frequency is clearly observed. Multiple and more intense harmonics as airspeed progresses can be seen. Particularly, for airspeeds over 40.0-45.0  $m/s$  one can see significant increase in LCO fundamental mode, which leads to higher frequency motions. Such condition is connected to the higher level of flow energy involved in the stall-induced excitation process.

#### 4. CONCLUSIONS

An analysis of non-linear aeroelastic responses for stall-induced oscillations of an airfoil in pitching moment is presented. The aeroelastic model is based on linear 1-*dof* structural dynamics in pitching coupled with a dynamic stall aerodynamic model, thereby allowing realistic higher angles of attack motions in low speed flow fields. The dynamic stall model is given by Beddoes-Leishman semi-empirical approach (Leishman and Beddoes, 1989) and NACA0012 parameters.

The modeling has been effective to capture the stall-induced loading fluctuations responsible to lead the aeroelastic system to high angle of attack LCO. LCO has manifested itself after a system bifurcation from stable equilibrium condition at approximately 23.8  $m/s$ . This airspeed establishes the minimum condition the flow energy provides to the onset of LCO at high angles of attack. As airspeed increases the fundamental frequency of LCO also tend to increase, because of more energy involved in the flow field. All LCO range in the aeroelastic system responses has also demonstrated to be stable ones.

#### 5. ACKNOWLEDGEMENTS

The authors acknowledge the financial support of CNPq (grant 303314/2010-9) and FAPESP (grants 2012/00325-4 and 2012/08459-1).

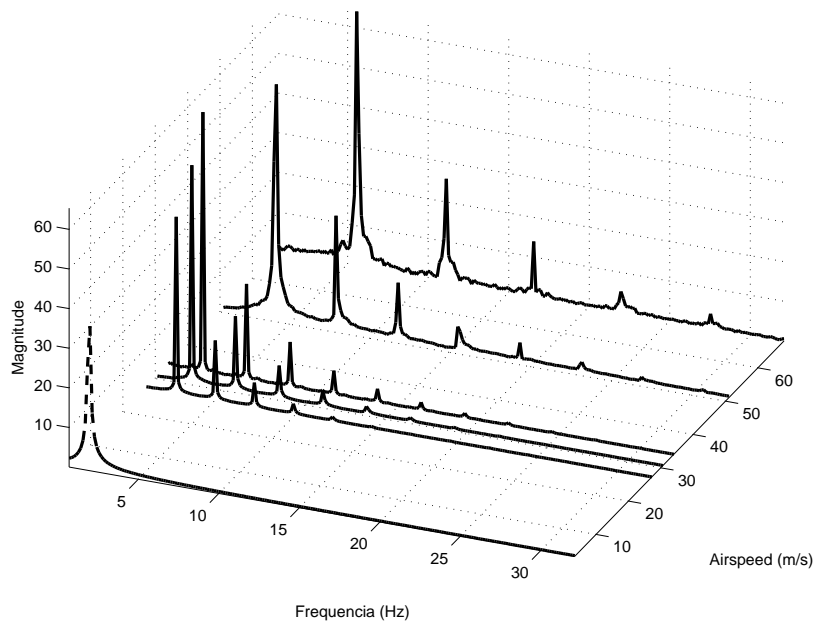


Figure 5. Power spectra evolution with respect to airspeed ( $\alpha_0 = 20^\circ$ ).

## 6. REFERENCES

- Anderson, J.D., 1991. *Fundamentals of aerodynamics*. New York: McGraw-Hill.
- Beddoes, T.S., 1976. "A synthesis of unsteady aerodynamic effects including stall hysteresis". *Vertica*, Vol. 1, pp. 113–123.
- Beddoes, T.S., 1982a. "Practical computation of unsteady lift". In *Eighth European Rotorcraft Forum*. Aix-en-Provence, France. Paper n. 2.3.
- Beddoes, T.S., 1982b. "Representation of airfoil behaviour". In *Specialists Meeting on Prediction of Aerodynamic Loads on Rotorcraft*. AGARD CP-334.
- Bielawa, R.L., 2006. *Rotary Wing Structural Dynamics and Aeroelasticity*. AIAA Education Series, USA, 2nd edition.
- Bisplinghoff, R.L., Ashley, H. and Halfman, R.L., 1996. *Aeroelasticity*. Dover, N. York, USA.
- Bramwell, A.R.S., Done, G. and Balmford, D., 2001. *Bramwell's Helicopter Dynamics*. 2nd edition.
- Burton, T., Sharpe, D., Jenkins, N. and Bossanyi, E., 2001. *Wind Energy Handbook*. John Wiley & Sons, Ltd.
- Chantharasenawong, C., 2007. *Nonlinear Aeroelastic Behaviour of Aerofoils Under Dynamic Stall*. Ph.D. thesis, Imperial College, London.
- Edwards, J.W. and Thomas, J.L., 1989. "Computational methods for unsteady transonic flows". In D. Nixon, ed., *Unsteady Transonic Aerodynamics*. AIAA, Vol. 120 of *Progress in Astronautics and Aeronautics*, pp. 211–261.
- Etkin, B. and Reid, L.D., 1996. *Dynamics of Flight: Stability and Control*. John Wiley & Sons, Inc., USA, 3rd edition.
- Fung, Y.C., 1955. *An Introduction to the Theory of Aeroelasticity*. Dover, New York, USA.
- Hansen, M.H., Gaunaa, M. and Madsen, H.A., 2004. "A Beddoes-Leishman type dynamic stall model in stat-space and indicial formulations". Technical Report Riso-R-1354(EN).
- Hansen, M.O.L., 2008. *Aerodynamics of Wind Turbines*. Earthscan, London, 2nd edition.
- Kantz, H. and Schreiber, T., 2004. *Nonlinear Time Series Analysis*. Cambridge University Press, Cambridge, 2nd edition.
- Leishman, J.G., 2006. *Principles of Helicopter Aerodynamics*. Cambridge University Press, 2nd edition.
- Leishman, J.G. and Beddoes, T.S., 1989. "A semi-empirical model for dynamic stall". *Journal of the American Helicopter Society*, Vol. 34, pp. 3–17.
- Mahajan, A.J., Kaza, K.R.V. and Dowell, E.H., 1993. "Semi-empirical model for prediction of unsteady forces on an airfoil with application to flutter". *Journal of Fluids and Structures*, Vol. 7, pp. 87–103.
- Marques, F.D., 1997. *Multi-Layer Functional Approximation of Non-Linear Unsteady Aerodynamic Response*. Ph.D. thesis, University of Glasgow, Glasgow, UK.
- McCroskey, W.J., 1982. "Unsteady airfoils". *Annual Review of Fluid Mechanics*, Vol. 14, pp. 285–311.
- Silva, W.A., 1993a. "Application to nonlinear systems theory to transonic unsteady aerodynamic responses". *Journal of Aircraft*, Vol. 30, No. 5, pp. 660–668.
- Silva, W.A., 1993b. "Extension of a nonlinear systems theory to general-frequency unsteady transonic aerodynamic responses". In *AIAA-93-1590-CP*. pp. 2490–2503.

D. A. Pereira, R. M. G. Vasconcellos and F. D. Marques  
Assessment of non-linear aeroelastic behavior of an airfoil vibrations in dynamic stall

- Tarzanin Jr., F.J., 1972. "Prediction of control loads due to blade stall". *Journal of the American Helicopter Society*, Vol. 17, No. 2, pp. 33–46.
- Thwaites, B., 1960. *Incompressible Aerodynamics*. Oxford University Press.
- Tobak, M. and Chapman, G.T., 1985. "Nonlinear problems in flight dynamics involving aerodynamic bifurcations". In *AGARD Symposium on Unsteady Aerodynamics. Fundamentals and Applications to Aircraft Dynamics*. Göttingen, West Germany. Paper 25.
- Tobak, M. and Pearson, W.E., 1964. "A study of nonlinear longitudinal dynamic stability". NASA TR R-209.
- Tran, C.T. and Petot, D., 1981. "Semi-empirical model for the dynamic stall of airfoils in view of the application to the calculation of responses of a helicopter blade in forward flight". *Vertica*, Vol. 5, pp. 35–53.

## 7. RESPONSIBILITY NOTICE

The authors are the only responsible for the printed material included in this paper.